

Measurement of Wind Waves and Wave-Coherent Air Pressures on the Open Sea from a Moving SWATH Vessel

MARK A. DONELAN

Rosenstiel School of Marine and Atmospheric Science, University of Miami, Miami, Florida

FRED W. DOBSON

Bedford Institute of Oceanography, Fisheries and Oceans Canada, Dartmouth, Nova Scotia, Canada

HANS C. GRABER

Rosenstiel School of Marine and Atmospheric Science, University of Miami, Miami, Florida

NIELS MADSEN

National Water Research Institute, Environment Canada, Burlington, Ontario, Canada

CYRIL MCCORMICK

Rosenstiel School of Marine and Atmospheric Science, University of Miami, Miami, Florida

(Manuscript received 13 December 2004, in final form 13 January 2005)

ABSTRACT

The design and implementation on a Small Waterline Area Twin Hull (SWATH) vessel of a complete system for measuring the directional distribution of wind waves and the concomitant fluctuations of air pressure and wind speed immediately above them are described. Data taken with the system on board the Canadian Coast Guard Ship *Frederick G. Creed* during the 1999 Shoaling Waves Experiment (SHOWEX) are used to calculate the wave-supported fluxes of momentum and energy between the air and the sea.

1. Introduction

This paper describes a seagoing measurement system designed to operate from a Small Waterline Area Twin Hull (SWATH) vessel at speeds of $5\text{--}8\text{ m s}^{-1}$ (10–16 kt). The system consists of a set of aluminum structures on which are mounted wave elevation, air pressure, wind vector, ship motion, turbulent and mean wind, and air and sea temperature sensors, all connected by cable to a central shipboard data acquisition system.

The unique features of this apparatus are (a) its use of laser elevation gauges for wave sensors, allowing an array of air pressure and wind speed sensors to be kept

close to the sea surface and obviating the need for water penetration by any of the critical sensors, and (b) its deployment on a stable, dynamically controlled platform capable of remaining relatively steady in roll and pitch in sea states up to Beaufort 5 while following the vertical motion of the dominant wind waves. These features allow, for the first time, direct measurements (i.e., the pressure–wave slope correlations) of the wave-supported momentum flux from a moving vessel in the open ocean. The apparatus was deployed during the 1999 Shoaling Waves Experiment (SHOWEX) on board the SWATH vessel CCGS *Frederick G. Creed*.

The design and operation of the system and some preliminary results are presented in this paper. Section 2 describes the experimental apparatus, section 3 describes the measurements and the method of their taking, section 4 outlines the data analysis, and sections 5 and 6 give some preliminary results and conclusions.

Corresponding author address: Mark A. Donelan, RSMAS, University of Miami, Division of Applied Marine Physics, 4600 Rickenbacker Causeway, Miami, FL 33149-1098.
E-mail: mdonelan@rsmas.miami.edu

2. Apparatus

a. SWATH vessel

The SWATH vessel CCGS *Frederick G. Creed* (Fig. 1) is a catamaran 20.4 m long and 10 m wide with a draft of 2.6 m and displacement of 75 metric tons. Twin diesel engines contained in the two underwater sponsons drive the ship at speeds up to 9 m s^{-1} . During SHOWEX, to minimize vibration on the bow mast and boom, she was run at speeds between 5 and 7 m s^{-1} . At speeds greater than 5 m s^{-1} the attitude of the vessel is controlled from the bridge using fins on the inner side of both sponsons. The movements of the fins themselves are controlled by a hardware/software feedback system that carries out the orders from the bridge-mounted control panel. With this system the mean pitch and roll of the vessel can be accurately controlled. Because the ship responds in heave to the longer, higher waves (i.e., waves with lengths comparable to the ship's length and longer), it is possible, in significant wave heights up to 2 m, to maintain the mean heights of fast-response air pressure and wind sensors much closer to the sea surface than would be possible on an ordinary displacement vessel.

b. Boom

The boom (Fig. 2), constructed of tubular aluminum, is designed to provide a lightweight yet stable platform for all instruments and accessories. It is secured parallel

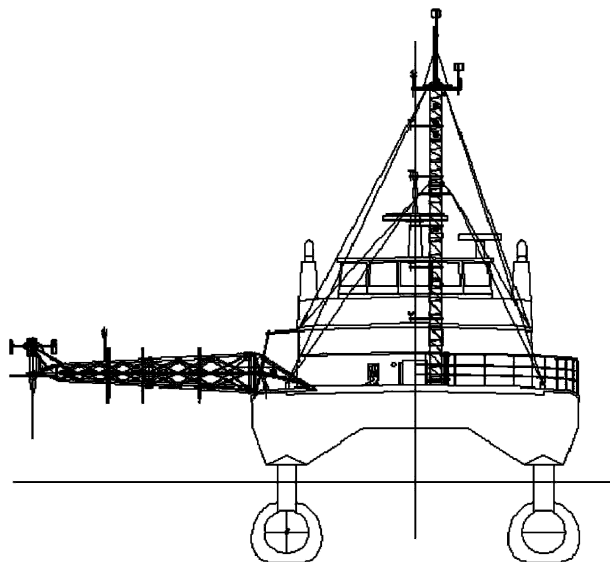


FIG. 1. Elevation drawing (from right ahead) of the SWATH vessel CCGS *Frederick G. Creed*, equipped with the SHOWEX bow mast and boom. Horizontal line is mean water level. Scale: The sonic anemometer at the top of the instrument mast is 14.3 m above the water.

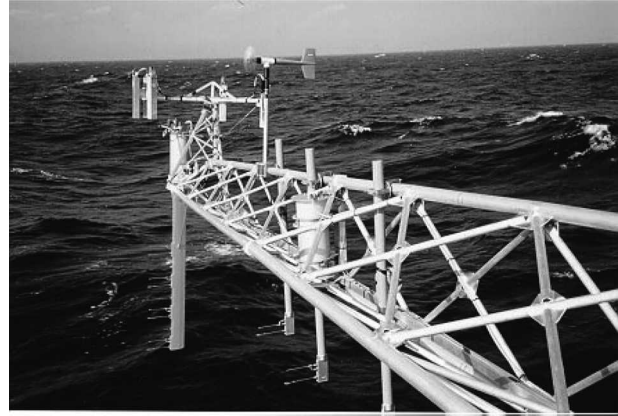


FIG. 2. Boom deployed from the starboard side of CCGS *Frederick G. Creed* during SHOWEX. The spar at the outer end of the boom that holds the vertical array of Elliott pressure sensors and Pitot and hot-film wind speed sensors (see Fig. 3) is in its working position at the tip of the boom. The array of laser altimeters is mounted immediately above the spar. The three fixed vertical inboard spars hold extra Elliott and Pitot sensors to measure the effect of the airflow blockage of the ship on the measurements. A fast-response propeller anemometer is mounted above the outer fixed vertical spar. The laser electronics container and the hydraulic control for the boom and spar retractor (not shown here) are mounted on the ship's deck just inboard of the spar.

to the vessel's railing during transport and instrument maintenance. A hydraulic actuator swings the structure outboard, perpendicular to the vessel's track, and it is then secured in position during a measurement session. The pivoting axis is canted so that the instrumentation is elevated to a working height in the transport/maintenance position and lowered to the measurement height in the operating position. The boom is designed so that, in the event of a collision, a locking pin will shear and a relief valve will permit release of the fluid from the hydraulic actuator back to the reservoir, allowing the structure to pivot back to the vessel's rail. This design feature was successfully tested on one occasion during SHOWEX when the boom tip touched the sea surface at 13 kt.

The deck-mounted frame that supports the boom requires two brackets welded at the edge of the deck and a mounting pad welded 1.75 m inboard. The deck below the pad is reinforced with a diagonal brace inside the vessel's hull.

c. Spar

At the end of the boom, 7 m from the starboard side of the ship, a retractable spar is attached (Figs. 2 and 3). It consists of a streamlined fiberglass post 2 m in length, topped by a cylindrical metal can, which houses the transducers and plumbing controls. The motion-

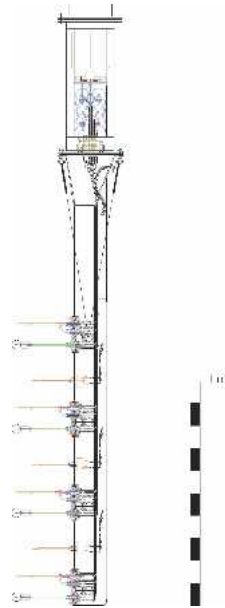


FIG. 3. Engineering drawing (elevation) of the fiberglass spar showing the locations of Elliott pressure and Pitot and hot-film wind sensors. Windward is on the left. There are four sets of Elliott pressure probes and Pitot probes and three holders between the pressure probes for a hot-film anemometer (in an X configuration for isolating the downstream component of the wave-supported Reynolds stress). Note that the Elliott sensors were operated with the disks in the horizontal plane; they are shown here in the vertical plane for illustrative purposes. The canister at the top contains the pressure transducers, plumbing and electronics for the array; the square box on top is a motion package. Note that the diaphragms of all eight pressure transducers are vertical in the x - z plane.

measuring package is bolted to the top of the can and thus responds to the local accelerations and rotations of the spar. The spar can be deployed or retracted hydraulically, folding inward so that it is horizontal and parallel to the boom. The spar is vertical in its normal mode of operation. However, if the tip of the spar touches the water it will swing backward (aft) against a pliable restraint of rubber cords. In moderate or high sea states this happened on several occasions per data run as we attempted to obtain pressure data as close to the surface as possible. The occurrence is clearly indicated in the records by sudden changes in the longitudinal and vertical accelerometers, which are rotated in the gravitational field.

d. Mast

The three-section aluminum mast (Figs. 4 and 5) rises 9.2 m above the deck. The top of the fiberglass sonic anemometer pole is 1.5 m higher. The mast is stayed by two sets of four-point guy wires. The base is bolted to



FIG. 4. Photo of the mast mounted at the bow of CCGS *Frederick G. Creed* during SHOWEX. There are two sonic anemometers mounted on the mast: the upper sonic anemometer is on the post at the top of the mast; the lower sonic anemometer is below and to port on a cross-arm, accompanied by a set of two fast-response air temperature sensors. Opposite the lower sonic on the same arm is a fast-response propeller anemometer. A motion package is mounted at the base of the upper sonic. A cup anemometer array can be seen just to starboard of the mast structure distributed over five heights. The top of the mast can be lowered to deck level by a hand-operated winch; there is a hinged joint above mast center. A cylinder containing dry nitrogen is lashed to the base of the mast; the gas is used to purge water drops from the Elliott and Pitot sensors.

the side of an existing winch platform. The mast is hinged at the top of the second section. The release of the aft upper-mast guy wires and securing latch permit the mast to be folded down on itself with a hand-operated winch. The folded tower facilitates installation and maintenance of the instruments and is also used during extended site-to-site transport.

e. Data acquisition system

The data acquisition system accepts signals from the various sensors and converts them to formatted ASCII

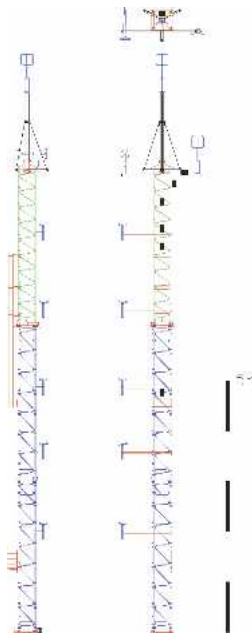


FIG. 5. Engineering drawing (elevation: view looking rearward at right, view from starboard on left, from above on top) of bow mast showing major instrument locations and hinge above center. The vertical pipe at the hinge is part of the mast-lowering mechanism.

numbers in tabular form on magnetic media. The main functional unit of the system is a PC-based computer with analog-to-digital converter (ADC) cards with differential signal input lines and a multiport RS232 card. Custom (Visual Basic) software was developed to manipulate these cards and format the generated data in computer memory. An additional housing contains sensor power supplies, connectors, antialiasing filters, and a very stable master clock. The master clock is used to synchronize the ADC and digital serial sensor sampling at a rate of 50 Hz. Asynchronous digital serial data from the shipboard positioning and hydrographic system are accepted and synchronized using the sample numbers generated by the master clock mechanism. After each sample run, the acquired dataset was copied from memory to hard disk files, and after several runs those files were written to CD-ROM.

f. Wave-sensing system

The wave-sensing system consists of an array of five laser altimeters and a 6 degrees of freedom motion-measuring package. The altimeters are pulsed infrared lasers designed for short-range (1–100 m) distance measurement (Riegl LD90–3100VHS-GF). The transmit and receive ports are separated by 2.5 cm, so that the optical alignment has to be optimized for the expected

range of measurement—in this case, 1–7 m. The lasers are mounted in a box just inside the railing of the ship at the base of the boom. They are connected via fiberoptic cable to their remote heads and these are arranged in two equilateral triangles (plan view) 2.8 m above the tip of the (deployed) boom. The apex of each triangle points directly forward (Fig. 6). Three lasers form the smaller triangle on a radius of 0.1 m about the centroid, which is itself the forward apex of the larger triangle on a radius of 0.75 m.

The centroid of the small triangle is directly above the sensing ports of the Elliott and Pitot pressure probes, so that these three altimeters yield the slope vector of the surface directly beneath the pressure probes. The larger triangle formed by any of the apexes of the small triangle (or their average) and the rearmost altimeters provides more sensitivity to slope of the longer waves. The pulsed lasers operate at 2000 Hz, and each measurement has an uncertainty of 2 cm. We record the altimetry data at 50 Hz per channel, combining up to 38 measurements (averaged) in each recorded point, thereby reducing the uncertainty to 3 mm. A successful range is realized only when some of the transmitted pulse is returned directly to the receiving optics. This requires a nearly normal specular point on the surface within the footprint—about a 3-cm-diameter circle. This sometimes does not occur, more frequently in light winds with a smooth swell running. As an indication of the reliability of each recorded average, we also record the average received power and the number (1–38) of successful measurements in each

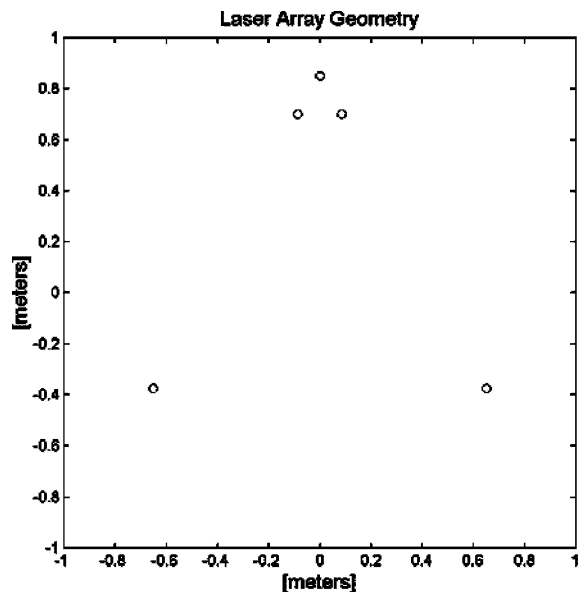


FIG. 6. Plan view of the locations of the laser altimeters in the laser directional wave array.

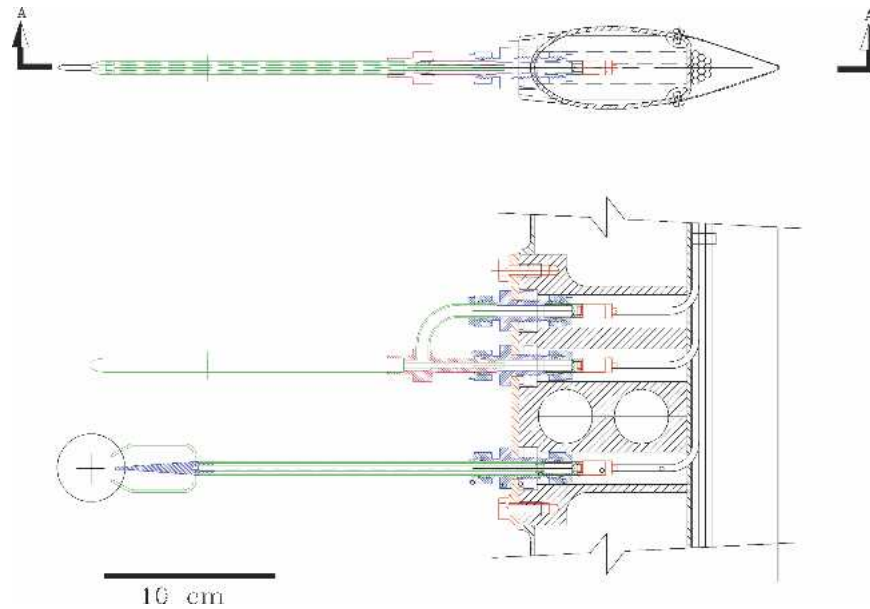


FIG. 7. Engineering drawing of the Elliott pressure probe and the Pitot probe mounted in their holders in the spar. Windward is to the left. The Elliott sensor is a thin disk, designed to measure only the static (i.e., ambient) pressure and to reject Bernoulli pressures caused by the flow around the probe at the 99.9% level. The pressure signals from ports on opposite sides of the disk are led to the sting via the two thin diagonal tubes, which also give the probe better twist resistance. The stalling airflow angle is about $\pm 12^\circ$. The Pitot probes measure the “dynamic” pressure ($\frac{1}{2} \rho U^2$, where ρ is the air density and U is the mean wind speed) and hence the wind speed, as long as the angle with the mean airflow is less than about 15° .

20-ms period. The received power may also provide a good measure of the incidence of whitecapping locally.

The lasers run asynchronously, but the danger of acceptance of received pulses from adjacent altimeters is nearly eliminated by gating the allowed return pulses to be consistent with the restricted range allowed. The remote heads are enshrouded in stainless steel jackets that serve to protect them from rain and spray and to collimate the receive beams and so limit the acceptance zone on the surface from which a return pulse may emanate. This further reduces the number of false returns from adjacent altimeters. The alignment of the transmit beams of the altimeters is critical to preserve the array pattern (Fig. 6) on the surface at various ranges. This was achieved in the laboratory and checked on the boom by means of a template of the form of Fig. 6. The (invisible) infrared beams were detected at night with infrared sensitive paper.

g. Air pressure sensing system

The air pressure sensing system consists of four pairs of sensors, each with one Pitot tube and one Elliott static pressure disk [see Figs. 2, 3, and 7 and Elliott (1972)].

For a complete description of the design and opera-

tion of the system see Donelan et al. (1999). The sensors are inserted with o-ring seals into receptacles in the spar (see Figs. 3 and 7), and the pressures they sense are conducted via stiff plastic tubing inside the spar to the canister above. Inside the canister are one 124-Pa [0.5 in. of water] full-scale MKS Baratron differential pressure transducer for each sensor, plumbing, including electrically controlled valves, and insulated air volumes (“backup volumes”) for each Elliott sensor. The valves are controlled remotely by the operator of the data acquisition system and allow for equilibrating the pressure in the backup volumes to exterior atmospheric pressure and subsequent purging of the small passageways of each sensor in turn with dry nitrogen to clear them of water droplets.

The Pitot sensors consist of a standard design [see, e.g., Prandtl and Tietjens (1934), section 126; details are given in Donelan et al. (1999)]. The total air pressure ($P_o + \frac{1}{2} \rho U^2$, where P_o is the static pressure and $\frac{1}{2} \rho U^2$ is the “dynamic” pressure associated with the airflow around the probe; ρ is air density and U the mean wind speed) is measured at the tip of the probe and led back to the positive port of the pressure transducer. The static pressure P_o only is measured at the side ports of the tube and led back to the negative port of the trans-

ducer. The difference recorded by the transducer is thus $\frac{1}{2} \rho U^2$, from which the relative airspeed is determined. The Pitot tubes used in SHOWEX measure the correct difference as long as the attack angle of the probe to the instantaneous wind direction is less than about 15° . The resolution and accuracy of the pressure measurement are 0.06 Pa (least significant bit) and 0.12 Pa. The small passageways in the Pitot tubes act as low-pass filters with a time constant of about 0.1 s.

The Elliott sensor [Elliott (1972); details specific to this configuration are in Donelan et al. (1999)] consists of a precisely shaped stainless steel disk, dished at the center and containing a 0.5-mm pressure port at the center of each face. To average the pressures on the two sides of the disk the pressure ports are not connected internally as they were in the original Elliott design; instead they are connected with two hypodermic needle tubes 1.5-mm outside diameter \times 0.18-mm-thick wall leading back to the sting about 5 cm behind (downwind from) the center of the disk. There they are joined to average the two port pressures. The average is more accurate because the length of the tubes to the sting can be equalized with higher precision. The Elliott shape is designed to reject 99.9% of the full dynamic pressure $\frac{1}{2} \rho U^2$ for attack angles up to 12° . This allows a determination of the static pressure with a noise level of less than 0.15 Pa at a mean wind speed of 15 m s^{-1} (the highest wind speed at which measurements were made during SHOWEX). To minimize the likelihood of stalling, the disks are oriented into the wind with their plane horizontal. In situations where there is a high probability of the probe touching the water surface, the disk may be oriented in a vertical plane. Each of the pressure sensing systems is equipped with an operator-controlled valve that allows entry of dry gas (in this case nitrogen) at a pressure of about 0.1 atmospheres (10^4 Pa) to blow out any water drops clogging the ports.

The probe delivers a measurement of static pressure back through the tubing to the positive side of the MKS transducer. The negative side of the transducer is connected through a short length of tubing to an insulated "backup" volume (a vacuum flask with an internal volume of 500 mL). For the first part of the field experiment (12–30 November) this backup volume was sealed. As the external air pressure varied with the passage of weather systems, an operator-controlled valve was used as needed to open the backup volume briefly and equilibrate its internal pressure to the outside. This required a level of vigilance that was difficult to maintain over repeated hour-long runs. Thus, for the remainder of the experiment (2–15 December) the equilibration of the backup volume was accomplished by

means of a slow leak to atmosphere (a hypodermic needle) with a time constant of 25 s.

h. Auxiliary instrumentation

In addition to the pressure and wave height measurement systems there were a number of auxiliary systems in place on the ship during SHOWEX. These are described below.

1) BOW MAST INSTRUMENTATION

The bow mast (Figs. 4 and 5) held instruments for measuring the mean and turbulent properties of the marine boundary layer and the momentum and heat fluxes through the sea surface. It was mounted just to port of center on the foredeck of the *Frederick G. Creed*. A motion package was mounted on the top of the mast. A Gill R3A sonic anemometer was mounted at the top of the mast on a 1.5-m fiberglass tube. The sonic anemometer provides accurate measurements of the three components of the mean and turbulent wind (downwind, crosswind, and vertical) and air temperature. Its height above the sea surface was 14.3 m. A vertical array of five cup anemometers (heights above the waterline of 4.75, 6.30, 7.85, 9.40, and 10.95 m) provided a check on the mean wind speed and an estimate of the effect on the wind speed measurements of the airflow distortion around the ship. During the period from 20 November to the end of the experiment, a Rotronics mean humidity and temperature sensor was attached to the mast at a height of 8.9 m. Data from the above instruments were logged on the same computer used for the instruments on the boom.

On a cross-arm immediately below the sonic mounting tube and 0.71 m to port of the ship's centerline another Gill R3A sonic anemometer was installed. Just inboard of the sonic anemometer, 0.7 m from the ship's centerline, was a small bracket containing two fast-response temperature sensors (VECO Fastip and Microbead). On the opposite (starboard) side of the cross-arm was mounted an R. M. Young AQ fast-response (distance constant 1.6 m) propeller anemometer, 0.7 m from the ship's centerline (the top anemometer in the cup array mentioned above) and 12.4 m above the waterline. Data from these sensors were logged separately. They were used to estimate the mean wind and temperature and the wind stress and heat flux through the sea surface. To cross-link the upper and lower turbulence systems, both systems logged a common timing signal.

For both sonic anemometers and the cup anemometers the manufacturer's calibrations were used for wind sensitivity; the sonic anemometer "zero wind"

measurement was made with the anemometers (each in turn) inside an anechoic tube. The R. M. Young anemometer was calibrated with a constant-speed motor drive to within 1% in mean wind speed. The fast-response temperature sensors were calibrated to within $+0.05^{\circ}\text{C}$ in a constant-temperature bath.

2) SUBMERGED PITOT TUBE

The ship's starboard sponson (see Fig. 1) was fitted with a bolting flange and penetrating tube to accommodate the installation of a submerged Pitot tube and mean water temperature sensor on the sponson's centerline axis. For details see Thwaites et al. (2000). Water speed and temperature data were logged separately on a third computer with a time/date stamp for subsequent integration into the complete dataset. The temperature sensor was calibrated to within $+0.1^{\circ}\text{C}$ during the field experiment against a "bucket thermometer" (a mercury-in-glass thermometer) measuring the temperature of sea surface water recovered in a bucket.

3) MARINE WAVE RADAR

A standard marine X-band (9.41 GHz) radar was mounted on the starboard side of the ship's bridge deck at a height of about 7 m above the sea surface. The radar is set at a 1-km range with a short pulse of 50 ns and repetition rate of 1300 Hz in order to record the sea clutter. It digitizes to 8-bit depth and records one 360° scan every 0.5 s to Exabyte tape. The radar is calibrated radiometrically to ± 0.2 dB. It is capable of making measurements of wave period (± 1 s), direction ($\pm 10^{\circ}$), wave height (± 0.3 m), and wind speed (± 2 m s^{-1}). With good ship's navigation data, detailed information can be derived on the adherence of the observed wave fields to the theoretical wave dispersion relation. The radar data were logged with time stamp and ship's navigation data to a separate (fourth) computer. The radar ran almost continuously throughout the data-gathering period and produced useful data for mean wind speeds greater than 4 m s^{-1} .

3. The SHOWEX measurements

The experiment was set in the shoal areas off the U. S. Army Corps of Engineers Field Research Facility (FRF) at Duck, North Carolina, about 32 km north-northwest of Cape Hatteras. The overall measuring period was from the beginning of September to the end of December 1999. The goals of the measurement program were to evaluate the interaction of wind waves and swell with the wind and with the sea bottom, the propagation characteristics of the waves, and the modi-

fication of the wave field by a shoaling bottom. The instruments chosen to do this work were selected to reveal wave characteristics (particularly directional characteristics) and the exchange of momentum and energy between winds, waves, and currents; between waves, the sea bottom, and currents; and among the waves themselves.

A number of data buoys were deployed by seven observational "teams" in an array offshore from the FRF extending from the beach to National Oceanic and Atmospheric (NOAA) buoy 44014, stationed at the edge of the continental shelf 88 km offshore. Included in the list were directional wave buoys, meteorological buoys, water and bottom-turbulence buoys, bottom-mounted acoustic Doppler current profilers, and three multispar [air-sea interaction spar (ASIS)] buoys (Graber et al. 2000) for determining the air-sea fluxes of heat and momentum. More detailed coverage of the area within the array was provided by a SWATH vessel (CCGS *Frederick G. Creed*) and four research aircraft. The aircraft used a variety of optical and radar techniques to sense the conditions at the sea surface (and in some cases at the sea bottom) as well as make standard measurements of the turbulent winds and air-sea fluxes in a variety of meteorological and sea state conditions. Only the measurements on the SWATH vessel are described in detail here. The ship was used to (a) provide a stable environment for the pressure-wave correlation measurements of wave-supported momentum and energy exchange between the winds and the waves, (b) make simultaneous measurements of the total air-sea momentum and heat fluxes and the directional characteristics of the waves, and (c) "fill in" areas not covered by the buoy arrays. In addition, advantage was taken of the presence on the ship of a multibeam mapping sonar system (SimRad E-1000) to make a detailed survey of the sea bottom at scales down to 100 m in a 6 km \times 6 km box near the center of the buoy array. The inner area of the buoy array was also covered by an HF radar system that was used to measure mean surface currents, winds, and wave parameters on a 1 km \times 1 km grid three times per hour.

4. Data analysis

a. Wave measurements with the laser array

The laser altimeters produce a digital string every 20 ms including the average range and amplitude and number of the successfully received signals (up to 38) of the previous 40 transmissions at 2000 Hz. The averaging and recording are done during pulses 39 and 40.

This digital string is recorded at 50 Hz by the computer and added to the analog records from some 52 other sensors. The altimeters are free-running, run asynchronously, and cannot be triggered by the computer; consequently, there may be some “slippage” in the registration of these digital data with respect to the analog stream. We determined that the slippage or shift in the data was linearly related to the number of bytes remaining in each altimeter’s buffer at the end of each second. This was carefully checked by means of the sharp interruption of the laser path with a rotating arm, whose rotation was measured by a potentiometer and recorded in the analog stream on the computer. Subsequently, the byte count in the output buffer was used to correct the registration of the digital streams from the laser altimeters.

The laser altimeters measure the distance to the surface from the moving and tilting boom. Consequently, the motion of the remote heads must be measured and appropriate corrections made to yield the elevation of the surface at the five points indicated in Fig. 6 along the path of the SWATH ship. The motion of the end of the boom was measured with a Systron-Donner (6 degrees of freedom) Gyro Cube. This device contains a triplet of orthogonal accelerometers and a triplet of orthogonal rotation rate sensors. These were carefully calibrated in the laboratory, the former by stepped rotation in the gravitational field and the latter by rotation at 0.2, 0.5, 1, 2, and 4 Hz using a precise linear “follower” to drive the rotation of a pivoted arm at whose pivot the Gyro Cube was attached. The transformations required to obtain along-track elevations of the surface from the shipborne laser altimeters are described in Drennan et al. (1994).

There were a total of 60 runs in which the boom was deployed and the lasers and their buffer contents recorded. The drop-out rate was the primary criterion for acceptance of a particular laser record. There were 37 cases in which all five lasers were acceptable and an additional 10 cases in which three or four lasers functioned well, including the base of the large array and one of the lasers at its apex. Therefore, in 47 cases both components of the surface slope could be determined, on a scale of a meter and longer, for correlation with the pressure measurements.

b. The Elliott pressure sensors

1) CALIBRATION

There are a number of calibrations to be done before the pressure measurement system can be relied upon to make accurate measurements of the static pressure

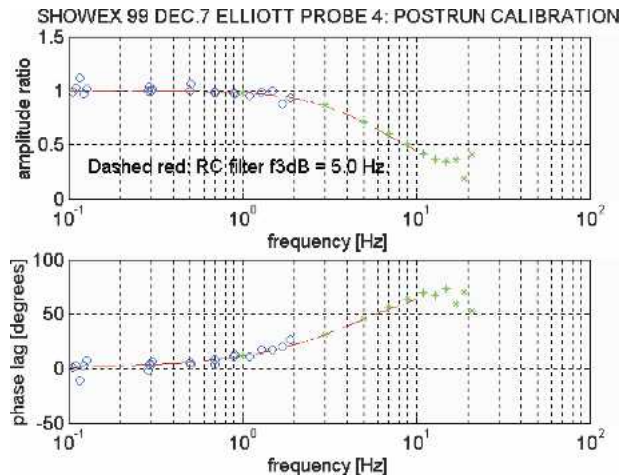


FIG. 8. Typical amplitude and phase calibration of an Elliott pressure sensor. The two sets of symbols (o, *) present the response function determined from triangular waves of two separate base frequencies (0.1 and 1 Hz). The dashed lines are the response function of a simple low-pass filter.

near the sea surface from a moving platform. First, the movements of the probe must be determined with a motion package—in this case a Systron-Donner Gyro Cube system. The vertical accelerations of all enclosed vertical air columns in the system generate pressure fluctuations that must be allowed for. Second, the vertical motion of the pressure sensor in the mean vertical air pressure gradient must be allowed for when correlating the pressure with the wave slope. Because the tubing in the Elliott sensor is narrow (the typical internal diameter of the passageways is about 0.2 mm), the probe acts as a low-pass filter to the incoming air pressure signals. The time constant of this filter must be allowed for in correcting the measured pressure signal and the effects of the vertical acceleration of the air passages on the measured pressure signal. Figure 8 shows a typical calibration. The calibration is accomplished by inserting the Elliott disk attached to its sting into a hollow cylinder with an internal volume of about 2 L that is driven at the other end with a radio speaker (Donelan et al. 1999). The speaker is actuated by a triangle wave from a signal generator. This excites odd harmonics, and by suitable choice of run length (= integer number of periods of the triangular wave), the output of the system is a response function consisting of a series of spectral lines (Fig. 8).

2) CORRECTION OF THE PRESSURE SIGNAL FOR ACCELERATION AND FREQUENCY RESPONSE

This describes the physical assumptions and the associated procedures that convert the pressure signals

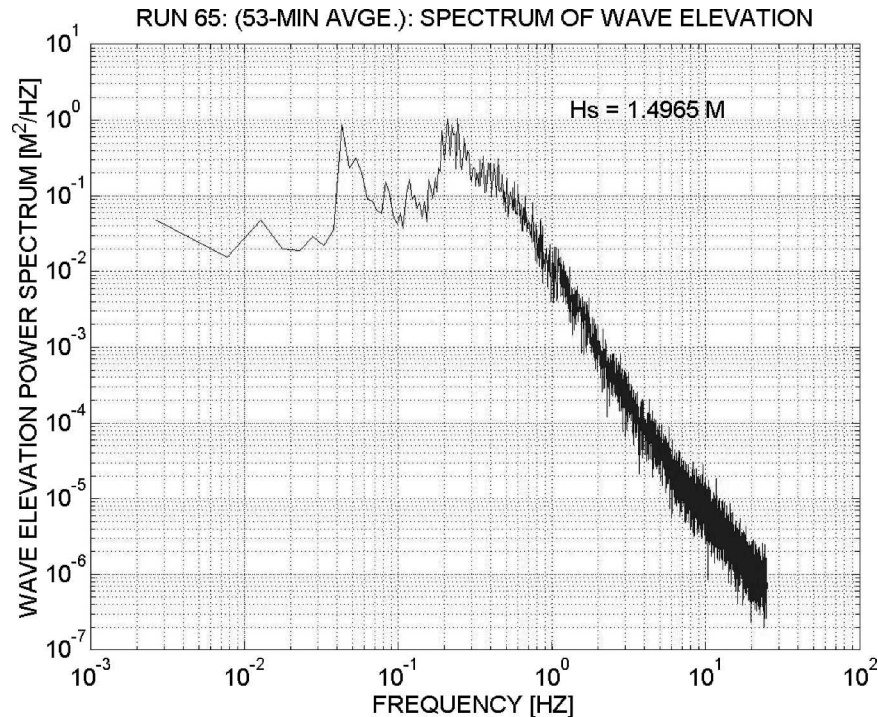


FIG. 9. Power spectrum of wave elevation from SHOWEX run 65. The wave elevation signal is the average of the three laser height gauges used to calculate the pressure-slope cross-spectrum (see Fig. 12); vertical ship motion has been allowed for. The frequencies are frequencies of encounter; they have not been corrected for the Doppler shift introduced by the ship's speed (about 6 m s^{-1}). The sea peak encounter frequency is at 0.21 Hz (the intrinsic frequency is about 0.14 Hz); the peak at 0.042 Hz is from a 0.3-Hz wave system moving with the ship.

(voltages from the MKS transducers recorded by the SHOWEX logging system) into calibrated and phase-corrected air pressures at the entrances to the Elliott sensor orifices. The procedures include initial conversion of volts to pressure measured at the MKS transducer and conversion of the measured pressures to pressures outside the Elliott orifice. Full corrections are made for the effects of the vertical acceleration of the sensor plus tubing as measured by the boom motion sensor (vertical acceleration) signal α_z .

(i) *Runs made up to 1 December 1999: Sealed backup volume*

From the start of the SWATH measurements until the end of November the pressure sensing system was operated with the backup volume sealed. To prevent the sensor from drifting out of the range of the A/D converters, valves were provided that allowed the operator, as necessary, to open briefly the backup volume of each sensor in turn, equilibrating its internal pressure with the mean air pressure at the time. The corrections

for the frequency response of the Elliott sensors (see Fig. 8; time constant about 0.2 s) and the acceleration of the air enclosed within the vertical parts of the tubing between the sensor and the transducer are made as follows:

$$p_o = p_M + L\rho\alpha_z \quad (1)$$

$$p_a = F^{-1}(p_o). \quad (2)$$

First, the pressure p_o just inside the Elliott sensor is calculated as the sum of the pressure p_M measured by the MKS transducer and the pressure $L\rho\alpha_z$ generated by the vertical acceleration α_z of the column of air enclosed in the connecting tube of (vertical) length L . The time series of the pressure p_o is then corrected for the known amplitude and phase response of the Elliott sensor (Fig. 8; represented by the filter operation, F) to compute p_a , the pressure outside the sensing disks.

After the Elliott sensor pressures are converted to the desired pressures outside the sensing disks, one more correction must be applied. As the boom and the

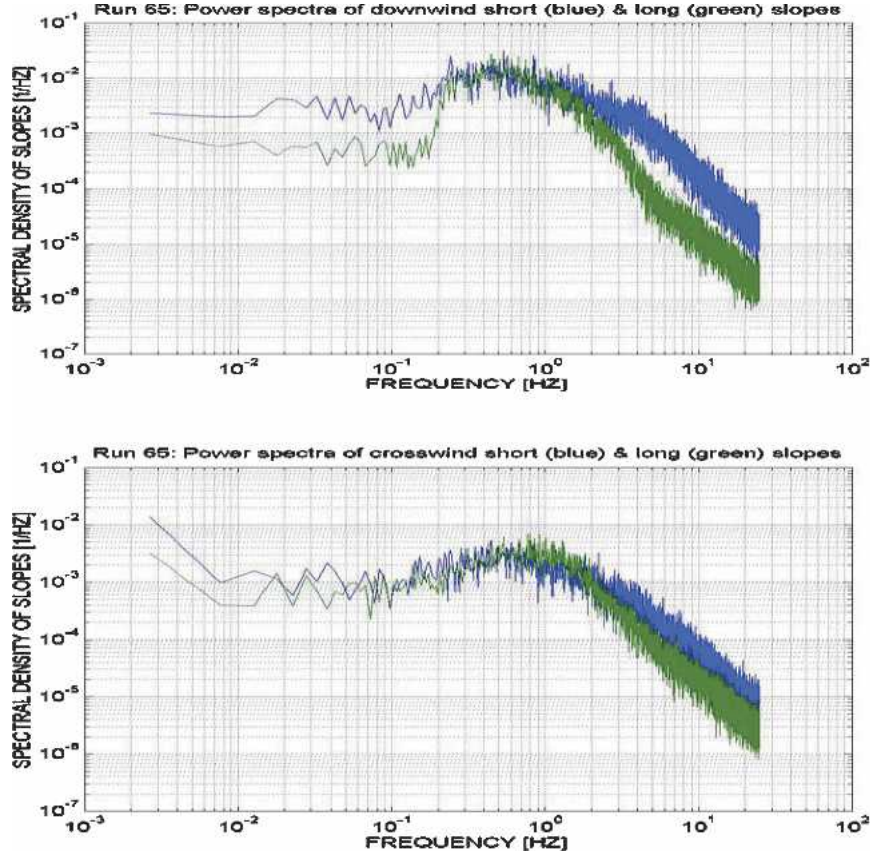


FIG. 10. Downwind and crosswind slope spectra from the small (blue) and large (green) triangles. Note the roll-off of the green curves due to the spatial filtering of the larger array.

spar containing the Elliott sensors is moved vertically by ship motion, the sensors register changes ($= \rho gh$) due to their motion in the mean vertical pressure gradient, where h is the vertical displacement of the boom. The displacement h is determined by performing a double integration on the boom vertical acceleration. This pressure is added (since the vertical pressure gradient is negative) to the measured pressures to give p_{ac} , the true air pressure outside the Elliott sensors:

$$p_{ac} = p_a + \rho gh. \quad (3)$$

(ii) *Runs made after 1 December 1999: Backup volume with slow leak to atmosphere*

The outside pressure is p_a , the pressure on the front (positive pressure) side of the MKS diaphragm is p_f , the pressure in the backup volume (and therefore on the back side of the MKS diaphragm) is p_b , and the pressure in the tubing just inside the Elliott disk is p_o . The MKS transducer measures the pressure difference $dp = p_M = p_f - p_b$.

The basic physics is as follows. Inside the tubing leading to the Elliott disk,

$$p_o = p_f + \rho L \alpha_z \quad (4)$$

$$p_o - p_b = [(p_f - p_b) + \rho L \alpha_z] = p_M + \rho L \alpha_z \quad (5)$$

$$p_o = p_M + \rho L \alpha_z + p_b, \quad (6)$$

where L is the vertical length of accelerated tubing and α_z is the vertical acceleration of the vertical length of tubing between the Elliott probe and the MKS transducer [see (i) above].

An iterative solution is called for, since the only knowns are p_M, α_z , and the time constants of the backup volume leak and the Elliott sensor. To obtain the “first guess” pressure p'_a outside the Elliott sensor, p_o is calculated from $p_M + \rho L \alpha_z$ (i.e., the MKS back pressure p_b is ignored) and corrected for the effect of the low-pass filter of the Elliott sensor (represented by the filter operation F) to give

$$p'_a = F^{-1}(p_o). \quad (7)$$

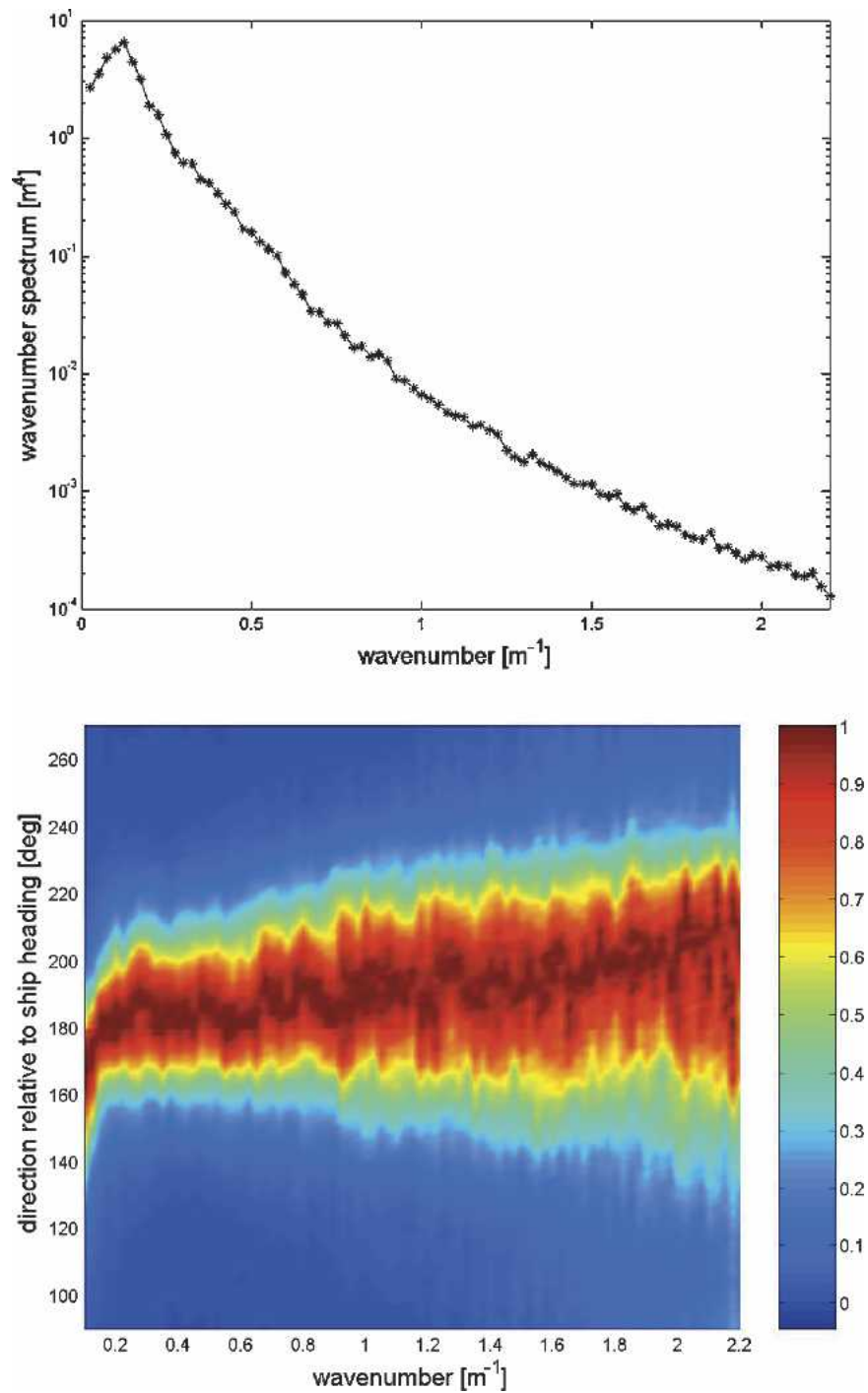


FIG. 11. Wavenumber directional spectra for run 65. (top) A slice of the wavenumber spectrum in the direction of the ship's track. (bottom) The spreading of wave energy. The directional distribution at each wavenumber is normalized by its peak.

The backup volume pressure p_b is then estimated by applying the low-pass filter of the leak into the backup volume (represented by the filter operation G) to p'_a . A new estimate of p_a is obtained from the sum of p'_a and

$F^{-1}(p_b)$, the pressure behind the diaphragm corrected for the effect of the Elliott sensor low-pass filter. Then p_a and p_b are iterated to close the solution; convergence occurs within three iterations:

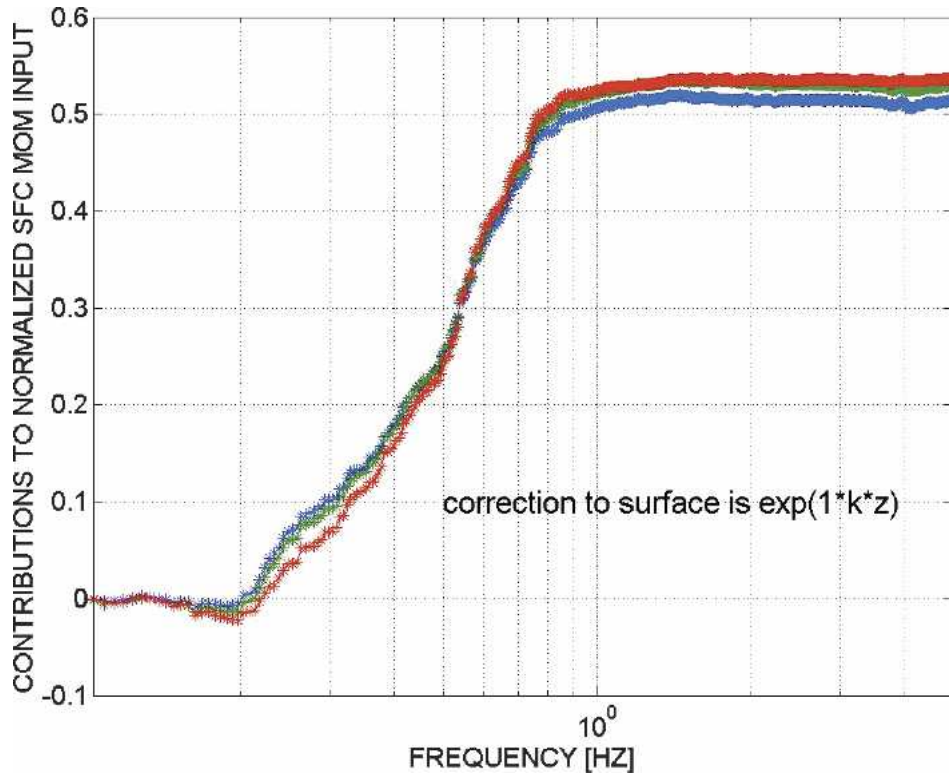


FIG. 12. Cumulative sum of spectral contributions to the wave-supported momentum flux for SHOWEX run 65. The contributions from each of three Elliott pressure probes has been corrected to the sea surface by multiplying contributions by $e^{\chi kz}$, where χ is a constant near 1 [the mean χ from Snyder et al. (1981) is 0.86], k is the wavenumber determined from the laser array, and z is the mean height of the Elliott probes above the sea surface. The blue curve is from the bottom Elliott probe, at a height of 1.3 m above the surface, the green curve is from the middle probe at 1.7 m, and the red curve is from the upper probe at 2.1 m.

$$\begin{aligned}
 p_b &= 0; \text{ (first guess)} \\
 p_o &= p_M + \rho L \alpha_z + p_b \\
 p'_a &= F^{-1}(p_o) \\
 p_a &= p'_a \\
 p_b &= G(p_a) \\
 p_a &= p'_a + F^{-1}(p_b) \tag{8}
 \end{aligned}$$

(iterate last two steps).

The remaining correction, to give the “true” air pressure p_{ac} outside the probe, allows for the vertical displacement h of the boom holding the Elliott sensor in the mean air pressure gradient:

$$p_{ac} = p_a + \rho gh. \tag{9}$$

5. Results

We present the results from a single data run, run 65 (1850–1950 UTC 6 December 1999) as an example of

the power of the instrument system and associated analysis procedures to determine the pressure–wave correlation spectra, and from them the momentum transfers from the wind to the sea surface waves.

The spectrum of encounter of the surface elevation measured by the laser system in run 65 is given in Fig. 9, while the spectra of downwind and crosswind slopes from both the small and large triangles are given in Fig. 10. The altimeters of the large triangle have been used to calculate the wavenumber directional spectrum using the wavelet directional method (WDM) of Donelan et al. (1996), as shown in Fig. 11. In Fig. 12 the momentum fluxes contributed by the pressure–wave slope correlations have been normalized by $\rho(u_*)^2$, where the friction velocity u_* has been determined from sonic anemometer measurements of the total momentum flux, or wind stress (= 0.012 Pa). This indicates that the measured wave-supported stress is a significant fraction ($>1/2$) of the total momentum flux into the sea surface. Note that the measured wave-supported stress is determined from the product of pressure (extrapolated to

the surface based on measurements at two heights) and the local wave slope. The wave-coherent pressure perturbations decay exponentially with height z (normalized by wavenumber k) [$p_{ac} = p_{sfc} \exp(-\chi kz)$] so that perturbations due to shorter waves are not discernible above the turbulent pressure fluctuations. The wave-supported stress vector due to waves long enough to provide coherent pressure fluctuations at height z is given in spectral form by

$$\tau_w = \mathbf{i} \int [\text{Co}(f)]_{p_{ac}\eta_x} e^{\chi kz} df + \mathbf{j} \int [\text{Co}(f)]_{p_{ac}\eta_y} e^{\chi kz} df, \quad (10)$$

where \mathbf{i} , \mathbf{j} , are unit vectors and η_x , η_y are surface slopes, in the downstream and cross-stream directions; $\text{Co}(f)$ is the frequency cospectrum of pressure, p_{ac} with slope. Figure 12 illustrates the cumulative sum of the downstream component of τ_w . Consequently, the fraction of the total stress due to wind-wave interaction (the wave-supported stress) shown in Fig. 12 is a lower limit.

6. Conclusions

With a relatively stable platform such as a SWATH vessel, careful design, and comprehensive data analysis, it is feasible to make accurate measurements at sea of air pressure-wave slope correlations, wave directional spectra, and other wave properties.

A system for measuring wave directional information and wave-supported momentum and energy fluxes in the open sea from a moving ship has been designed, implemented, and proven in the field in the fall of 1999 during SHOWEX in the waters off Duck, North Carolina, near Cape Hatteras. In this paper we have demonstrated the methodology of these delicate measurements, illustrated the importance of careful calibrations, and given some examples of the results. It remains to carry out more complete analyses of the extensive datasets to improve our knowledge of wavenumber spectra of wind waves and the form and strength of the wind forcing in both deep and shoaling conditions. This endeavor is currently under way.

Acknowledgments. We gratefully acknowledge the assistance of Messrs. James Bull, Joe Ford, Robert Reid, Harry Savile, Klavs Davis, Joe Gabriele, and Ken Hill of NWRI in the design and implementation of the fittings for the SWATH vessel. Steve Peck of DFO

Headquarters in Ottawa gave generously of his time to ensure we got the vessel charter through the bureaucracy. M. Lamplugh and personnel from the Canadian Hydrographic Service, working under contract, joined the ship for two 2-day periods to provide precision sounding data for SHOWEX. R. Anderson and M. Scotney assisted with the BIO part of the field experiment, and M. Rebozo with the RSMAS component. Prof. J. R. Buckley of the Royal Military College, Kingston, Ontario, provided the wave radar. The shipboard observations were onerous, calling for long hours “at the controls”; invaluable help was provided by Bob Anderson, Fabrice Ardhuin, Will Drennan, Tom Kinder, Nick Reul, Gene Terray, and Ian Young. The captains and crews of CCGS *Frederick G. Creed* provided invaluable help with the seamanship associated with using new equipment at sea. The personnel of the NOAA Atlantic Marine Laboratory, in particular its Facility Manager, Mr. Robert Lundy, in many ways facilitated our work during the ship’s stay at Norfolk, Virginia. Bill Birkemeier of the U.S. Army Coastal Research Station at Duck was our host and coordinated many of our multifarious activities at his station. This work was funded by the Coastal Dynamics Branch of the Office of Naval Research under Grants N00014-97-1-0348 to RSMAS and N00014-97-1-0809 to BIO.

REFERENCES

- Donelan, M. A., W. M. Drennan, and A. K. Magnusson, 1996: Nonstationary analysis of the directional properties of propagating waves. *J. Phys. Oceanogr.*, **26**, 1901–1914.
- , N. Madsen, K. Kahma, I. Tsanis, and W. Drennan, 1999: Apparatus for atmospheric surface layer measurements over waves. *J. Atmos. Oceanic Technol.*, **16**, 1172–1182.
- Drennan, W. M., M. A. Donelan, N. Madsen, K. B. Katsaros, E. A. Terray, and C. N. Flagg, 1994: Directional wave spectra from a SWATH ship at sea. *J. Atmos. Oceanic Technol.*, **11**, 1109–1116.
- Elliott, J. A., 1972: Instrumentation for measuring static pressure fluctuations within the atmospheric boundary layer. *Bound.-Layer Meteor.*, **2**, 476–495.
- Graber, H., E. Terray, M. Donelan, W. Drennan, J. Van Leer, and D. Peters, 2000: ASIS—A new air-sea interaction spar buoy: Design and performance at sea. *J. Atmos. Oceanic Technol.*, **17**, 708–720.
- Prandtl, L., and O. G. Tietjens, 1934: *Applied Hydro- and Aeromechanics*. Dover, 311 pp.
- Snyder, R. L., F. Dobson, J. Elliott, and R. B. Long, 1981: Array measurements of atmospheric pressure above surface gravity waves. *J. Fluid Mech.*, **102**, 1–59.
- Thwaites, F. T., E. A. Terray, and T. de Crisnay, 2000: A Pitot sensor for measuring near-surface turbulence. *Proc. Oceans*, **2000**, 981–986.